THERMAL INERTIA MODELLING FOR SOIL MOISTURE ASSESSMENT BASED ON REMOTELY SENSED DATA.

Beata Hejmanowska, research assistant, University of Mining and Metallurgy, Cracow, Poland
Stanisław C. Mularz, senior lecturer, University of Mining and Metallurgy, Cracow, Poland

Commission VII, Working Group 1

KEY WORDS: Remote_Sensing, Soil, Thermal, Surface, Model, Remote_Sensing Soil Mapping, Thermal Inertia Modelling, Soil moisture assessment.

ABSTRACT

After Pratt's. et al. (1980) the thermal inertia model have been used for soil moisture assessment of the bare soil surface. As an input data the model requires the digital images of soil albedo (A), diurnal temperature differences (ΔT) and also a set of geographical / meteorological data. For the study area (4 x 4 km) the data were collected during the two-level experiment consisted of an airborne remote sensing imagery and the simultaneously *in situ* measurements. After calibration procedure of the remotely sensed data the maps of thermal inertia and soil-moisture distribution on the test fields were generated. A good approach to the different data categories was achieved. A removal of the topographical effect using Digital Elevation Model (DEM) of the study area and Lambert's method was also tested.

1. INTRODUCTION

A suitable method for remote measurements of soil moisture is not elaborated as yet. It seems, on the base of the literature, that the suitable part of a spectrum for registration of a wet soil is thermal infrared. In the future it will be probably possible to use a microwave, but till now the property of this part of spectrum has not fully recognized for this purpose. The best method according to the soil water assessment using remote sensing data, is based on the thermal inertia model. The thermal inertia value (P) depends on thermal conductivity (k), heat capacity (c) and density (ρ) of the ground :

$$P = \sqrt{k\,c\,\rho}$$

The inertia can be calculated using not only this directly measured soil parameters but also on the base of remote sensing data. For this method it is necessary to know values of the following remotely measured variables: the maximum diurnal temperature differences and albedo. The thermal inertia (P) can be calculated on the base of this input data using the numerical model taking into account meteorological conditions and geographical coordinates. Theoretical backgrounds of the soil thermal inertia model were given by H.S. Carslaw and J.C. Jeager (1953). Heat conducting within the ground is governed by the known heat diffusion equation. There are many ways to solve this heat diffusion equation. The results depend on boundary conditions and a chosen solution method. Many authors published own methods of thermal inertia modeling. It seems to be, that Pratt D.A. et. al. (1980) proposed the best one. They consider in the energy balance the energy provided to the ground (Sun radiation and sky radiation), and the energy given by the ground (radiation emitted by ground, sensible heat flux and latent heat flux).

Estimation of the water content on the bare soil surface was the main goal of the study presented. For this purpose the airborne / terrestrial experiment was performed. The following experimental data set was acquired:

- airborne panchromatic photos of the test area,
- series of airborne thermal images which corresponding to the maximum and the minimum diurnal temperature,
- data of *in situ* monitoring the soil temperature and water content,
- terrestrial thermal imagery of the selected part of the test area.

Example of topographical correction and its influence on the thermal inertia modeling is also presented. The method of calibration of the remotely sensed data and the results of testing of the thermal inertia model using a set of the experimental airborne data and real ground observation are also described.

The research was conducted within the project of the Polish Committee of Scientific Research (grant No 9 S605 019 06)

2. STUDY AREA AND DATA COLLECTION

The study area is located in the southern part of Poland near the Carpatian Foothills, approximately 50 km east of Cracow (Fig.1.). Considering the main purpose of this investigation, the two-level experiment was performed in the early spring-time of 1995 (2-3 May).

Remotely sensed data were collected over the 4.0 x 4.0 km study area within the rural region.

The airborne panchromatic photos of the study area have been taken at 2 o'clock p.m. on ILFORD HP5 PLUS film, using small-frame camera (70 x 56 mm).

The thermal infrared (TIR) imageries have been taken using the AGEMA THERMOVISION SYSTEM 780 which on-board registered the series of thermal images in digital format.

For measurement of the maximum diurnal temperature differences two thermal flights were done over the study area, the first about 2 o'clock p.m. and the second about 5 o'clock a.m. just before the sunrise.

1. The study area consists of several agriculture fields and the similar soil type - loess and loess-like. The four fields (A,B,C,D) were selected as the test areas for the *in situ* investigations (Fig.1.).

4. METHODOLOGY AND RESULTS

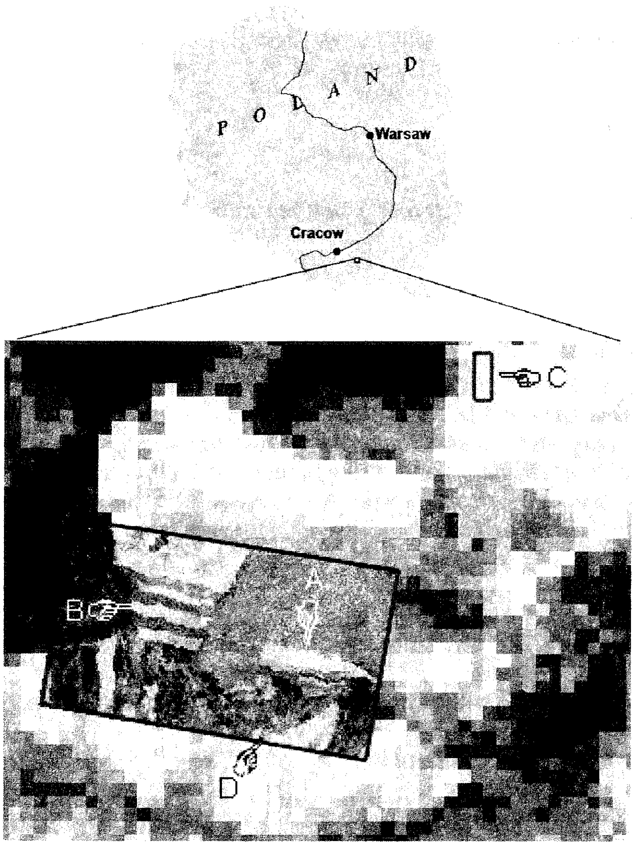

Fig. 1 The study area and test fields.

Finally, the following data set was obtained as the ground support for the remote sensing observations:

1. The results of soil temperature and soil moisture monitoring of the test fields. All the temperature measurements and the sampling for soil moisture determination, have been done simultaneously with the acquisition of the remotely sensed data. On the test field A a special system was installed for the automatic soil temperature measurements. Based on the two full cycles of these measurements the dynamic of the diurnal temperature changes of the soil has been evaluated. The water content of the soil samples was assigned by weighing method.
2. The terrestrial thermal imagery of the selected part of the test field A has been taken, mainly for the Bidirectional Radiation Distribution Function (BRDF) assessment in the thermal infrared region of the electromagnetic spectrum. For this purpose the thermovision camera was placed in the middle of the circle and the several thermograms have been registered looking towards and back of the incidence radiation. The sequence of the 18-th imageries were recorded on each of 20 azimuth direction (chosen thermogramms are shown on Fig.13) . As the results of the detailed analysis of remotely sensed data and *in situ* measurements, the field B has been selected as „sample area" for preprocessing the whole data set.

Thermal inertia modeling was performed for all of the test fields.

Panchromatic photos, in average scales (1:9000, 1:3000), was digitized with 600 dpi resolution, so 1 pixel on the image corresponds to 0.38 and 0.13 m on the terrain. Thermal radiation was digital recorded as an image of 80 columns and 90 rows, 1 pixel corresponds to 1.5 m.

Panchromatic and thermal images were initially preprocessed for adjustment to soil albedo and temperature distributions. The test fields are composed with loess and loess-like soils. On the base of the references and previous own research the albedo for dry loess was assumed as 0.33 and for wet 0.22. Thermal images was calibrated using ground temperature measurements. The temperature was changing, for sample area (field B), from 16 to 20 °C.

The thermal inertia modeling was performed on the preprocessed remote sensing data considering meteorological conditions and geographical co-ordinates as follows:

- latitude of the center of the test field: 50° N, longitude: 20 ° E,
- Sun declination:+16° , inclination: -0.8°,
- maximum diurnal temperature differences of the soil surface: 20 °C,
- range of the air temperature: 20 °C,
- average air temperature: 8 °C,
- average wind velocity: 1.1 m/s.

Image processing was carried out using the own computer software basing of the Pratt's et. al.(1981) theoretical background.

The last step was the finale soil moisture calculation.

Remote sensed data and *in situ* measurement collected for the test fields were statistically analyzed. Relationship between the following variables were considered in all possible combinations:

- soil moisture (m_b - hillocks of micro-relief, m_u - hollows of micro-relief-, m_s - soil surface),
- thermal inertia [TI - calculated on the base of Pratt's. et. al. (1981) model, TI_o - calculated from the simple equation: $(1-A)/\Delta T$],
- albedo - A,
- maximum diurnal temperature differences - ΔT.

Variance-covariance matrix for the test field B is shown bellow (Tab.2.)

	m_b	m_u	m_s	TI	TI_o	A	ΔT
m_b	1	0,71	0,56	0,78	0,62	-0,53	**-0,91**
m_u		1	0,45	**0,90**	0,87	-0,78	-0,84
m_s			1	0,42	0,13	-0,23	**-0,57**
TI				1	**0,94**	-0,92	-0,89
TI_o					1	**-0,94**	-0,72
A						1	0,63
ΔT							1

Tab.2. Variance-covariance matrix.

The relationship between albedo, maximum diurnal temperature differences, thermal inertia and soil surface is presented on Fig.3.

The analysis of the results shown in Tab.2. and on Fig.3. allow to state that:

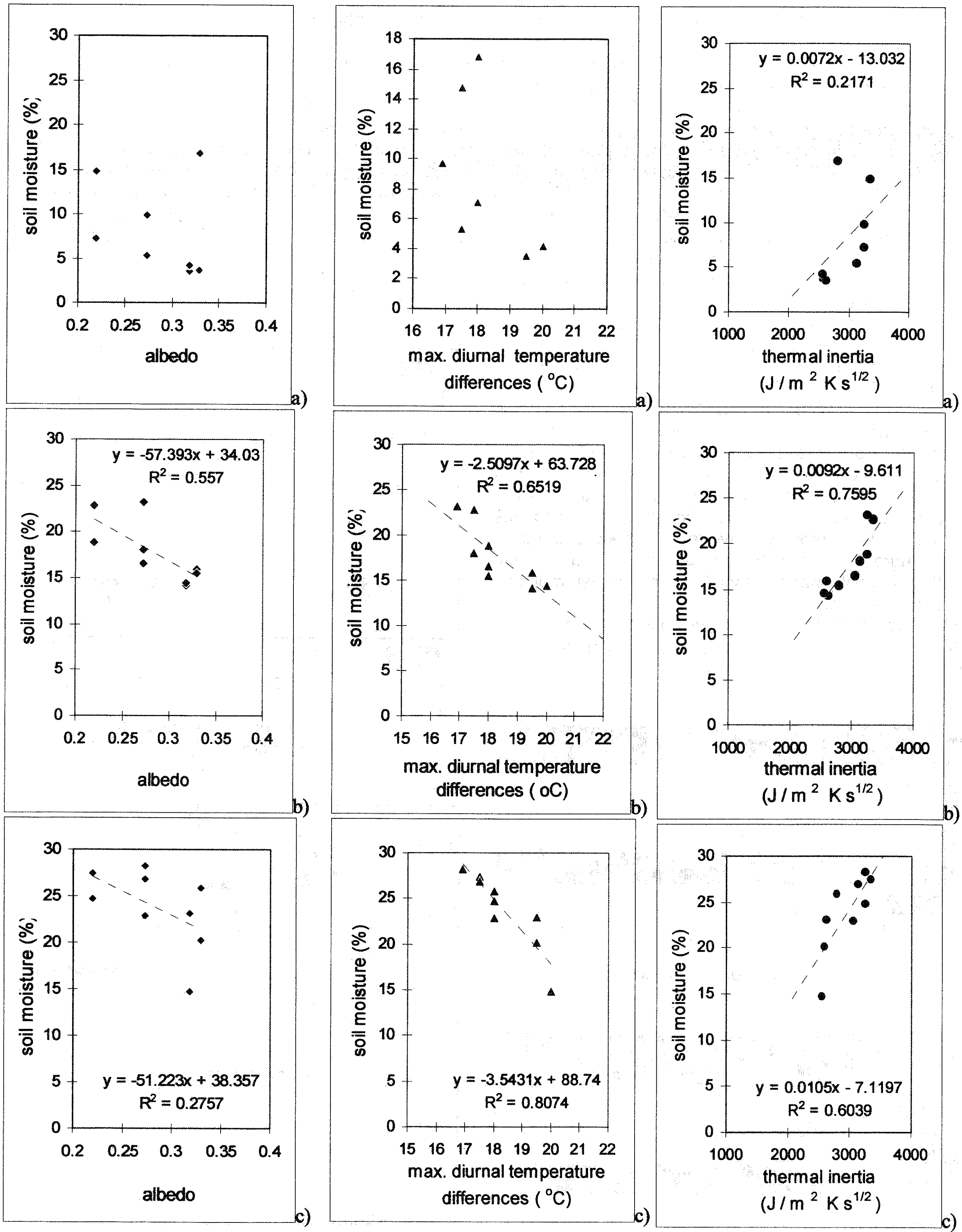

Fig.3. Relationship between albedo, maximum diurnal temperature differences, thermal inertia and soil moisture, a) soil surface, b) hillocks of micro-relief, c) hollows of micro-relief.

1. The best relationship between analyzed variables (A, ΔT, P) and soil moisture (m_b, m_u, m_s, was obtained for the hillocks of soil micro-relief. The most significant correlation was achieved between the thermal inertia (TI) , calculated from Pratt's. et. al. (1981) model and soil moisture of hillocks of micro-relief (m_u). The similar relationships between soil moisture and temperature of the soil were reported by Idso (1975) and Zielińska (1984)
2. The regression coefficient for relationship between soil moisture and thermal inertia is significant (R^2 = 0.7595), while between maximum diurnal temperature differences is less (R^2 = 0.6519) and between albedo is the lowest (R^2 = 0.557).
3. Unexpectedly bad correlation was noticed for albedo and soil moisture. This was probably caused by the sampling method, which was not representative enough for the variability of the observed albedo levels. Another words, the number of the soils samples for water content evaluation was insufficient to fit all the albedo changes, especially because of the influence of the micro-relief of the soil surface. This was clearly visible on the original panchromatic airborne photos, (Fig.8). The problem, how to take the samples that could be representative for an albedo and a temperature distribution for the particularly image scale, the different images resolution and proper mapping time is still open.

Below are some examples of the input data: albedo A, (Fig.4),maximum diurnal temperature differences ΔT, (Fig.5).

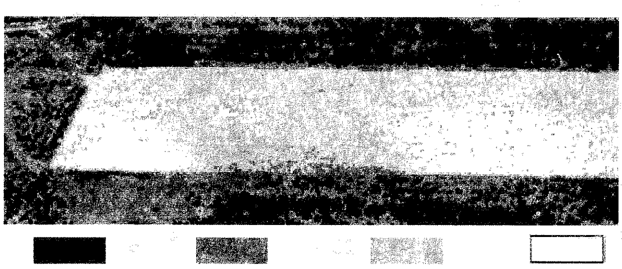

Fig. 4. Albedo of the test field B.

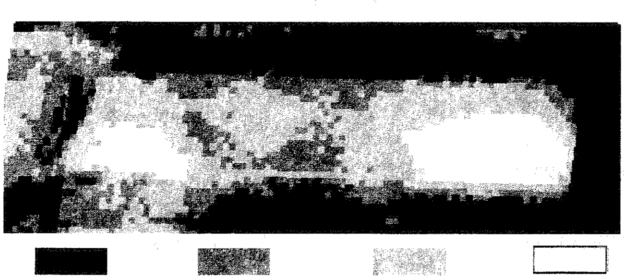

Fig.5. Maximum temperature differences [°C], (field B).

The result of processing: thermal inertia P, and finally soil moisture distribution for one of the test field (B) are presented on Fig.6 and Fig.7.

4.1. Topographic effect

Thermal inertia modeling needs calibration of remote sensed images to albedo and temperature distribution. The level of electromagnetic energy registered in remote sensing techniques depends also on the terrain topography. Variation of albedo and temperature might to be caused by topographic effect. Correction method is

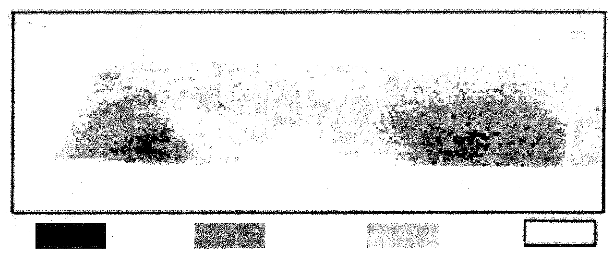

Fig.6. Thermal inertia [$J / m^2 K s^{1/2}$], (field B).

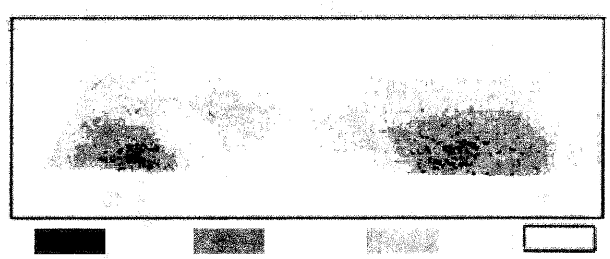

Fig.7. Moisture of the soil surface (hillocks of micro-relief) [%], (field B).

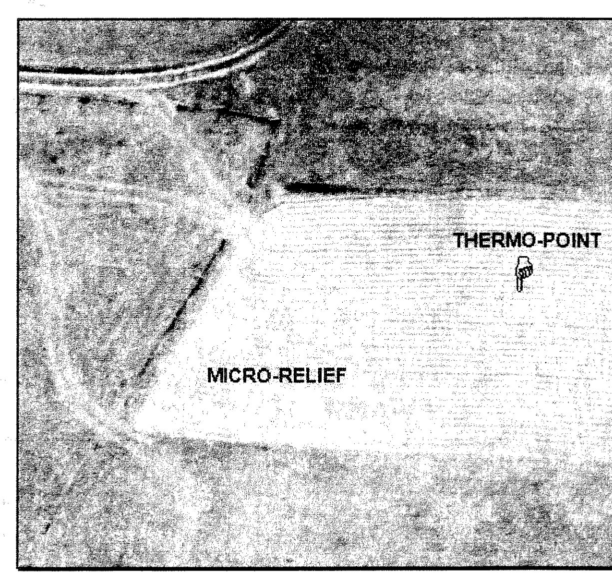

Fig. 8. Enlargement of the panchromatic photos (field B).

based on the assumption that the required radiation level should be equal to the radiation, reflected from horizontal surfaces. It means, that after transformation we should obtain the radiation distribution similar as is observed for the flat terrain. For correction of the topographical effect the Bidirectional Reflection (or Radiation) Distribution

Function has to be known. This photometric function depends on microscattering properties of the individual surface elements and macrostructure of the soil surface (Hapke B. W. 1963). Macrostructure can be classified as smooth, corrugate or porous. Microscattering properties can be divided into three general types: forward- , isotropic- or backscattering.

To remove negative topographic effect we need to know the solar illumination conditions on slope surfaces. The procedure of removing topographical effect from remote sensing data usually consists of following stages:

1) Calculation of slope and exposure of the soil surface for each pixel of DEM.
2) Evaluation of the solar zenith angle and azimuth for horizontal surface at the moment of registration. For this purpose it is necessary to know:
   - Sun declination and inclination depended on a day and an hour of the registration,
   - geographical co-ordinates of the research area: latitude and longitude of the center of test area.
3) Evaluation of illumination angles of sloping surface (solar zenith angle and azimuth) for each pixel on the base of data:
   - slope and exposure of the surface for each pixel,
   - solar zenith angle and azimuth of the horizontal surface.
4) Generation of the correction coefficient image using known BRDF.
5) Multiplication the raw images by the correction coefficient images.

Many Geographical Information Systems (GIS) allow to calculate slope and azimuth from DEM, some of them have an option to remove topographical effect using the simplest BRDF, basing on the Lambert's formula. The Lambert's method was criticized cause over correction of the slopes with north exposures, (Smits G.H. et. Al. 1980). There are also another developed of theoretical models (for example: Hapke B.W., 1963, Kimes D.S and Kircher J.A. 1981, Cierniewski.J. 1991).

The test area was topographically diversified with elevation differences ranging from 215 to 280 m above see level and slopes from 0° to 28°. Corresponding incident angle (solar zenith angle) vary from 30° to 80°.

For testing the different BRDF it was necessary to prepare a special computer program. Two examples of the correction coefficient images draped on DEM are shown on Fig.9, and Fig.10.

Mentioned above BRDF models were worked out for visible range of electromagnetic spectrum. There is a question: is it possible to use them for thermal range? Does the thermal radiation depend on registration direction or not?

During the thermal inertia modelling for soil moisture assessment the problem connected with the calibration of the thermal images has also appeared. Temperature of the soil surface strongly depends on the exposures and of the slope range. The slopes looking North are of course cooler of those looking South. In the thermal inertia modelling for soil moisture evaluation the soil surface temperature for areas of the similar water content should be on the same level and should not be dependent on the surface exposures.

To check this question some initial measurements were made. On the Fig.12 an example of the terrestrial thermal image of filed D is shown. Filed D has a northerly exposure and slope of 10°. The right part of field D was wet (approx. 18%), left part was dry (approx. 9%). The thermal measurements of field D were compared to the temperature obtained for flat part of field B. The results are shown in Tab.9.

Area	Field B (flat part)		Field D		
	m.	T	m	T_o	T_c
1	14%	16 °C	9%	10.5 °C	17.9 °C
2	19%	14 °C	18%	8.7 °C	14.7 °C

Tab. 9. Thermal measurements of field D compared to the temperature for the flat part of field B *[m - soil moisture, T - temperature of field B, T_o- temperature of field D (raw data), T_c- modified temperature of field D (assuming that surfaces are heating according to the cosines of incident angle)].*

It is clearly visible, that applying correction procedure the temperature levels (T_c) of field D are comparable to the temperature levels (T) of field B and now could be used for thermal inertia modelling.

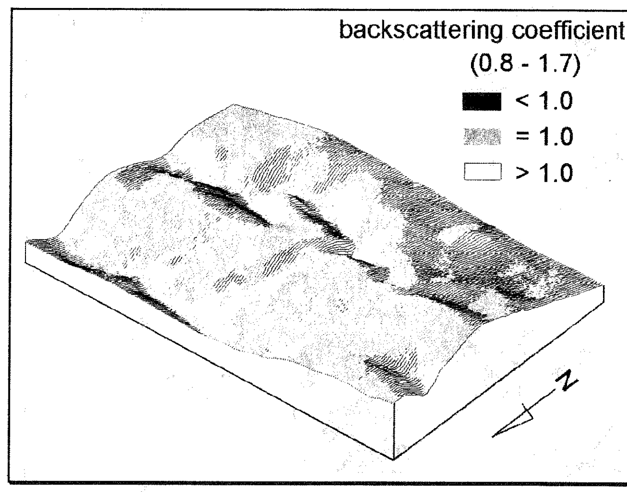

Fig. 10. Backscatterig coefficient image.

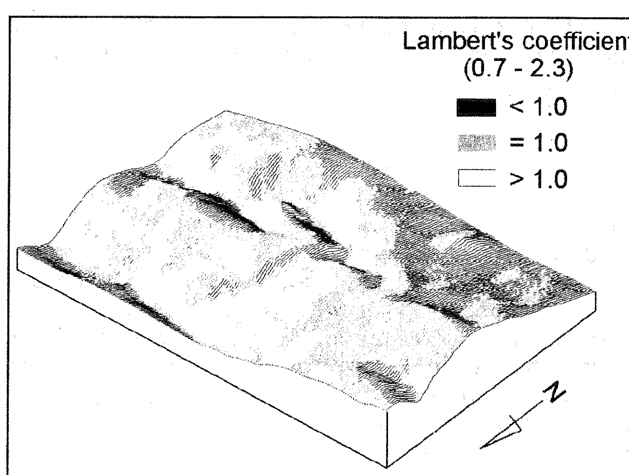

Fig.11. Lambert's. coefficient image.

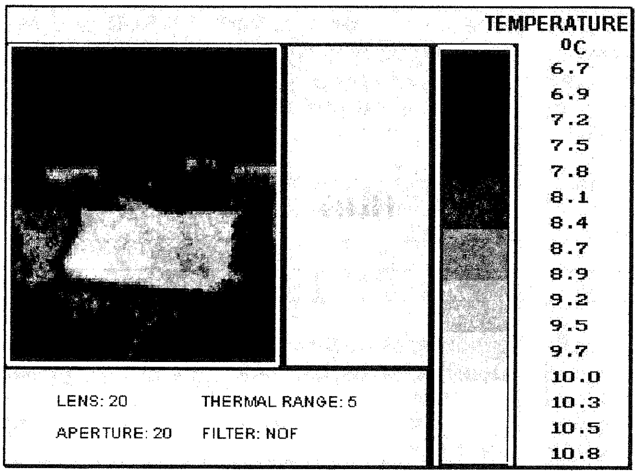

Fig.12. An Example of the terrestrial thermal image, (field D).

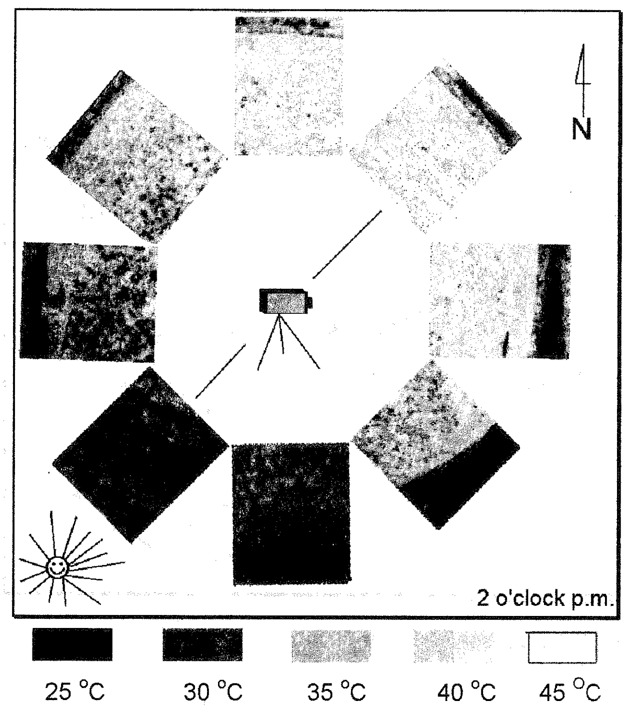

Fig.13. Influence of the geometry (direction of registration and Sun main plane) on terrestrial temperature measurement.

CONCLUSIONS

This study presents the attempt to apply thermal inertia model and remote sensing data for soil moisture mapping over the study area of the homogeneous soil type and diversified topographically as well as from the point of view of agricultural use. For thermal inertia modeling the main data set should be consisted of the geographical and meteorological data, the remote sensing imagery and some of the *in situ* measurements (soil temperature and soil moisture) for the calibration of the diurnal temperature differences and the soil moisture evaluation procedure.

The research reported here also indicated that the removal of the topographic effect based on DEM and Lambert's. method is very advisable, especially on the morphologically diversified areas. As expected, some problems and inconveniences connected with the field works organization and remote sensing data pre-processing, were observed. It occurs mainly because the remote sensing observations and field measurements have to be done simultaneously at precisely defined and very short time periods, for the maximum and the minimum soil diurnal temperature. It should be stressed that sufficient numbers of the ground control, and thermal points are required for geocoding and merging procedures.

The research suggests that an automatically mapping of the soil surface moisture is possible and seems to be very effective tool for the agriculture purposes: planning and management. Knowledge about soil-water conditions is very important in the planning of the structure crops, prediction of yield and also implementation of a conservation program for most agricultural soil.

6. REFERENCES

Cierniewski, J., 1991. Specular - diffuse model of soil bidirectional reflectance in the visible and near - infrared range. Remote sensing of Environment.

Hapke, B.W., 1963. A Theoretical photometric function for the lunar surface, Journal of Geophysical Research, 68 (15): pp. 4571-4586.

Hejmanowska B., 1991 Thermal inertia modeling of soil, Geodesy and Cartography vol. XL, No 2, pp. 215-231,

Kimes, D.S., Kirchner, J.A., 1981. Modeling the effects of various radiant transfer in mountains terrain on sensor response. IEEE Transactions on Geoscience and Remote Sensing, GE-19 (2): pp. 100-107.

Smith, J.A., Lin, T.L., Ranson, K.J., 1980. The Lambertian assumption and Landsat data. Photogrammetry Engineering and Remote Sensing, 46 (9): pp. 1183-1189.

Carslaw, H.S., Jeager, J.C. Conduction of heat in solid, Oxford, London, 1959.

Dąbrowska-Zielińska K., 1984. Research on the application of remote sensing for soil moisture analysis. Proceedings of the Inst. Of Geodesy and Cartography vol. XXXI, No1, pp. 43 -55

Idso S.B., 1975. The utility of surface temperature measurements for the remote sensing of surface soil water status, Journal Geophysical Research, Vol. 80, No 21. July 20,

Mularz S.C., Hejmanowska B., 1990. Digital processing of remotely sensed data for thermal inertia mapping. In International Archives of Photogrammetry and Remote Sensing, International Symp. Com. III of ISPRS, „Progress in data analysis", Wuhan, China, May 20-24.

Pratt D., Foster S.J., Ellyett C.D., 1980 A calibration procedure for Fourier series thermal inertia model, Photogrammetric Engineering and Remote Sensing, No 4, April., pp. 529-538,